Surge motion-induced dynamic inflow effects in floating offshore wind turbines

A State Prediction Model

Meng, Qingshen; Yu, Wei

**Important note**
To cite this publication, please use the final published version (if applicable).
Please check the document version above.

**PAPER • OPEN ACCESS**

# Surge motion-induced dynamic inflow effects in floating offshore wind turbines: A State Prediction Model

To cite this article: Qingshen Meng and Wei Yu 2024 *J. Phys.: Conf. Ser.* **2767** 062018

View the article online for updates and enhancements.

# Surge motion-induced dynamic inflow effects in floating offshore wind turbines: A State Prediction Model

**Qingshen Meng, Wei Yu**

Wind Energy Section, Flow Physics and Technology, Faculty of Aerospace Engineering, Delft University of Technology, Kluyverweg 1, Delft, 2629HS, Netherlands

E-mail: `Q.S.Meng@tudelft.nl, W.Yu@tudelft.nl`

**Abstract.** The impact of surge motion on aerodynamic unsteadiness in modern floating offshore wind turbines (FOWT) is a well-recognized phenomenon. When coupled with advanced controllers integrated into these turbines, it can lead to fluctuations in power output. This paper introduces a state-space model that incorporates dynamic inflow effects resulting from surge motion and a PID pitch controller. Additionally, an observation equation is formulated to predict the system power output. Through time series validations, the proposed state-space model demonstrates its ability to accurately capture power responses influenced by surge motions. The developed model serves as a valuable tool for the comprehensive analysis of FOWT, allowing for the exploration of the intricate interplay between unsteady aerodynamics, advanced control mechanisms, and power output.

## 1. Introduction

Amid rising energy demand and limited land, FOWT has gained focus on the existing alternatives in energy capturing. Yet, FOWT advancement faces inevitable challenges, particularly in power and movement control and state prediction [1]. Due to the complicated movements of FOWT caused by unpredictable wave and wind states, the power and load outputs can fluctuate [2], while wave dynamics, steady and unsteady aerodynamics, as well as advanced control, can participate in this process. In which the topic of dynamic inflow is becoming popular, especially when the FOWT is in surge motion. Experimental [3] and high-fidelity simulation [4] investigations are conducted by some researchers successively, revealing some interesting phenomena different from bottom fixed wind turbines. Besides, an analytical model is also given by Ref. [5] and is implemented in the typical Blade Element Momentum (BEM) theory. PID controller is generally adopted as the core module to regulate the rotor power output [2]. However, when it comes to the PID controller design and parameter optimization, the influence of steady and unsteady aerodynamics remains unable to be fully included [6]; this insufficiency could be placed in a prominent position. Better state prediction has also been a major concern in the past several years, for which power and loads are vital. Power and loads can be predicted utilizing the BEM theory with satisfying accuracy [7]. However, it fails to analyze the intrinsic mechanism between the FOWT motions, aerodynamic unsteadiness, advanced controller, and power production analytically. More deeply, some potential scientific issues are still unexplored, such as how the actuator disk influences the pitching ratio and power

production of the rotor, and inversely, how the pitching ratio influences the actuator disk, etc., and the current tool cannot perform these analyses. The above-mentioned issues prove the demand for a to-be-developed integrated model with explicit expressions.

This paper aims to develop an analytical model that can combine platform surge movement, dynamic inflow effect, and advanced PID pitch controller, as well as power production, within the state space framework. These aspects are typically assembled with nonlinear and implicit expressions, proving the potential and rationality of gluing up. A step forward, once these blocks are linearized into state space, their collaboration still seems to be reliable and even more straightforward, which encourages us to develop such a model. This model enables revealing the relation between these different aspects through off-diagonal elements in matrices, which can provide a novel insight into floating wind turbine dynamics. Previous nonlinear dynamic models are unable to achieve this quantitatively. From the perspective of mathematics, the model proposed in this paper successfully introduces both controller and dynamic inflow into state space simultaneously for the first time.

## 2. Model development
This section is dedicated to presenting the foundational theory underlying the PID controller and dynamic inflow model, alongside their respective linearizations. Additionally, an observation equation will be formulated to monitor the states of the FOWT. These individual equations are finally integrated within the state-space expression.

### 2.1. PID controller and linearization
#### 2.1.1. PID controller
The PID pitch controller employed in this study incorporates the benchmark model documented by the National Renewable Energy Laboratory [8], specifically developed for a 5MW wind turbine. Due to the linearization objectives, certain adjustments will be introduced.

The equation of motion for drivetrain degree of freedom can typically be given as:

$$\dot{\Omega} = (T_{aero} - N_{gear}M_{gen})/I_{rx} = L_1 \tag{1}$$

in which $I_{rx}$ is the inertia combines the rotor($I_{rotor}$) and generator($I_{gen}$):

$$I_{rx} = I_{rotro} + N_{gear}^2 I_{gen} \tag{2}$$

besides, $T_{aero}$ is the aerodynamic torque due to the spinning of the rotor: $T_{aero} = \int_0^R r \cdot dS$, $r$ is the radius of an element and $dS$ is the tangential force originating the torque. $M_{gen}$ is the torque of the high-speed shaft of the generator, it's assembled by timing the gear ratio $N_{gear}$.

Applying a traditional PID pitch controller, for which the target pitch angle $\beta_t$ can be determined using the following equation:

$$\beta_t = K_P N_{gear} \Delta\Omega + K_I N_{gear} \int_0^t \Delta\Omega \mathrm{d}t + K_D N_{gear} \Delta\dot{\Omega} \tag{3}$$

Eq.3 can be further expanded as:

$$\beta_t = K_P N_{gear}(\Omega - \Omega_0) + K_I N_{gear}(\Phi - \Omega_0 t) + 0$$
$$= K_P N_{gear}\Omega + K_I N_{gear}\Phi - K_P N_{gear}\Omega_0\left(1 + \frac{K_I}{K_P}t\right) \tag{4}$$

We assume that the target pitch angle should be completed within time step $\Delta t$, thus

$$\dot{\beta} = \frac{\Delta\beta}{\Delta t} = \frac{\beta_t - \beta}{\Delta t} = \frac{1}{\Delta t}\beta_t - \frac{1}{\Delta t}\beta \tag{5}$$

with $\beta$ being the pitch angle at the current time step.

Now isert Eq.4 into Eq.5, and the final mathematic expression can be drawn as:

$$\dot{\beta} = \frac{1}{\Delta t} K_P N_{gear} \Omega + \frac{1}{\Delta t} K_I N_{gear} \Phi - \frac{1}{\Delta t} \beta - \frac{1}{\Delta t} K_P N_{gear} \Omega_0 \left( 1 + \frac{K_I}{K_P} t \right) = L_3 \qquad (6)$$

Furthermore, by the geometric relationship, the first derivative of azimuth, denoted as $\Phi$, can be explicitly defined as:

$$\dot{\Phi} = \Omega = L_2 \qquad (7)$$

### 2.1.2. Linearization

Notably, it should be observed that the parameters in Eq. 1 encapsulate variables implicitly:

$$T_{aero} = T_{aero} \left( \Omega, \beta, u_{act}, U_{surge} \right), \quad M_{gen} = M_{gen} \left( \Omega \right) \qquad (8)$$

in which $u_{act}, U_{surge}$ represent actuator disk and platform surge velocity, respectively.

Therefore, the aforementioned equation can be extended through the utilization of a first-order Taylor's expansion, resulting in:

$$
\begin{aligned}
\delta\dot{\Omega} &\approx \frac{\partial L_1}{\partial \Omega} \delta\Omega + \frac{\partial L_1}{\partial \beta} \delta\beta + \frac{\partial L_1}{\partial u_{act,0}} \delta u_{act} - \frac{\partial L_1}{\partial U_{surge,0}} \delta U_{surge} \\
\delta\dot{\Phi} &= \delta\Omega \\
\delta\dot{\beta} &\approx \frac{\partial L_3}{\partial \Omega} \delta\Omega + \frac{\partial L_3}{\partial \Phi} \delta\Phi + \frac{\partial L_3}{\partial \beta} \delta\beta + \frac{\partial L_3}{\partial t} \delta t
\end{aligned}
\qquad (9)
$$

The partial derivatives can be further expressed in the following equations:

$$
\begin{aligned}
\frac{\partial L_1}{\partial \Omega} &= \frac{1}{I_{rx}} \left( N_b \int_0^R r \frac{\partial \mathrm{d}S}{\partial \Omega} - N_{gear} \frac{\partial M_{gen}}{\partial \Omega} \right), \quad \frac{\partial L_1}{\partial \beta} = \frac{1}{I_{rx}} N_b \int_0^R r \frac{\partial \mathrm{d}S}{\partial \beta} \\
\frac{\partial L_1}{\partial u_{act,0}} &= \frac{1}{I_{rx}} N_b \int_0^R r \frac{\partial \mathrm{d}S}{\partial u_{act,0}}, \quad \frac{\partial L_1}{\partial U_{surge,0}} = \frac{1}{I_{rx}} N_b \int_0^R r \frac{\partial \mathrm{d}S}{\partial U_{surge,0}} \\
\frac{\partial L_3}{\partial \Omega} &= \frac{1}{\Delta t} K_P N_{gear}, \quad \frac{\partial L_3}{\partial \Phi} = \frac{1}{\Delta t} K_I N_{gear}, \quad \frac{\partial L_3}{\partial \beta} = -\frac{1}{\Delta t}
\end{aligned}
\qquad (10)
$$

Several items necessitate further derivation: $\frac{\partial \mathrm{d}S}{\partial \Omega}$, $\frac{\partial \mathrm{d}S}{\partial \beta}$, $\frac{\partial \mathrm{d}S}{\partial u_{act,0}}$, $\frac{\partial \mathrm{d}S}{\partial U_{surge,0}}$, and $\frac{\partial M_{gen}}{\partial \Omega}$. Notably, the latter, $\frac{\partial M_{gen}}{\partial \Omega}$, signifies the slope depicted in the diagram in Fig.1. A comprehensive derivation for the rest items is provided in Appendix A.

### 2.2. Dynamic inflow engineering model and linearization

### 2.2.1. Dynamic inflow engineering model

The engineering dynamic inflow model developed specifically for a FOWT in surge motion [5] was implemented in this manuscript:

$$
\begin{aligned}
U_{\infty ref}(k) &= U_{\infty ref}(k-1)e^f + (U_\infty - U_{surge}) \left( 1 - e^f \right) \\
u_{act}(k) &= u_{act}(k-1)e^{-\frac{\Delta t}{\tau_{act1}}} + u_{qs} \left( 1 - e^{-\frac{\Delta t}{\tau_{act2}}} \right) \\
u_{str}(k) &= u_{str}(k-1)e^{-\frac{\Delta t}{\tau_{str}}} + u_{qs} \left( 1 - e^{-\frac{\Delta t}{\tau_{str}}} \right)
\end{aligned}
\qquad (11)
$$

in which $U_{\infty ref}$ is the reference unperturbed velocity of the wind used in the actuator disc model, $u_{act}$ is induction velocity at the location of the actuator, and $u_{str}$ is the stream tube induction
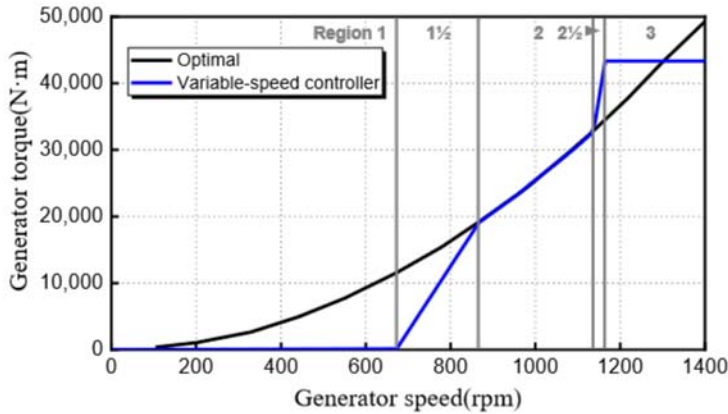
Figure 1: Determination of $\frac{\partial M_{gen}}{\partial \Omega}$

velocity. In addition, $U_\infty$ represents the incoming wind speed from the far field. The other variable definitions in the above equation can be found in Ref [5].

As the PID controller and structural dynamics are generally written in continuous state space format [9], the equation above can be further transferred into a continuous expression. Using $Z$ transformation, the equations can be transferred into $Z$ domain, and then using the relation $Z^{-1} = 1 - S\Delta t$ to rewrite the equations into $S$ domain, and finally using the inverse Laplace transformation to rewrite the equation into continuous format as:

$$
\begin{aligned}
\dot{U}_{\infty ref}(t) &= \frac{1}{\Delta t}\left(1 - e^{-f}\right)U_{\infty ref}(t) + \frac{1}{\Delta t}\left(e^{-f} - 1\right)(U_\infty - U_{surge}) = \mathcal{F}_1 \\
\dot{u}_{act}(t) &= \frac{1}{\Delta t}\left(1 - e^{\frac{\Delta t}{\tau_{act1}}}\right)u_{act}(t) + \frac{1}{\Delta t}e^{\frac{\Delta t}{\tau_{act1}}}\left(1 - e^{-\frac{\Delta t}{\tau_{act2}}}\right)u_{qs} = \mathcal{F}_2 \\
\dot{u}_{str}(t) &= \frac{1}{\Delta t}\left(1 - e^{\frac{\Delta t}{\tau_{str}}}\right)u_{str}(t) + \frac{1}{\Delta t}\left(e^{\frac{\Delta t}{\tau_{str}}} - 1\right)u_{qs} = \mathcal{F}_3
\end{aligned}
\tag{12}
$$

### 2.2.2. Linearization

Performing the linearization step by step, and assuming the time step is small enough, we can thus utilize the first-order Taylor's expansion for linearization:

$$
\begin{aligned}
\delta\dot{U}_{\infty ref}(t) &\approx \frac{\partial \mathcal{F}_1}{\partial U_{\infty ref}}\delta U_{\infty ref} + \frac{\partial \mathcal{F}_1}{\partial U_{surge}}\delta U_{surge} \\
\delta\dot{u}_{act}(t) &\approx \frac{\partial \mathcal{F}_2}{\partial U_{\infty ref}}\delta U_{\infty ref} + \frac{\partial \mathcal{F}_2}{\partial u_{act}}\delta u_{act} + \frac{\partial \mathcal{F}_2}{\partial u_{str}}\delta u_{str} + \frac{\partial \mathcal{F}_2}{\partial U_{surge}}\delta U_{surge} + \frac{\partial \mathcal{F}_2}{\partial \Omega}\delta\Omega + \frac{\partial \mathcal{F}_2}{\partial \beta}\delta\beta \\
\delta\dot{u}_{str}(t) &\approx \frac{\partial \mathcal{F}_3}{\partial U_{\infty ref}}\delta U_{\infty ref} + \frac{\partial \mathcal{F}_3}{\partial u_{act}}\delta u_{act} + \frac{\partial \mathcal{F}_3}{\partial u_{str}}\delta u_{str} + \frac{\partial \mathcal{F}_3}{\partial \Omega}\delta\Omega + \frac{\partial \mathcal{F}_3}{\partial \beta}\delta\beta
\end{aligned}
\tag{13}
$$

The partial derivatives that appear above require further derivation. However, due to constraints on the page, the detailed derivations are omitted. Nevertheless, the final expressions for these derivatives are provided in Appendix B.

### 2.3. Observation equation

The parameters under surveillance encompass critical aspects such as power output, thrust, torque, etc. Among these, power output holds particular significance and is observed by the following equation:

$$
P = \eta \cdot M_{\text{gen}} \cdot \left(\Omega_0 + \sum_{i=1}^{n}\delta\Omega_i\right) \cdot N_{\text{gear}}
\tag{14}
$$

where $\eta$ represents the efficiency factor, which accommodates for energy losses in the drive chain and is assumed to be 0.94. Furthermore, $N_{\text{gear}}$ stands for the gear ratio, with a specific value of 97 for the 5MW model.

### 2.4. Expressions in state space

As a result of the aforementioned derivations, the PID pitch controller and dynamic inflow model have been systematically linearized, and their expressions are assembled in Eq.15. Within this equation, the speed variation of surge motion is considered as one of the inputs, with $K_I N_{\text{gear}}\Omega_0$ representing the time-independent input. The matrix elements clarify the interactions among different variables.

$$
\begin{Bmatrix} \delta\dot{\Omega} \\ \delta\dot{\Phi} \\ \delta\dot{\beta} \\ \delta\dot{U}_{\infty ref} \\ \delta\dot{u}_{act} \\ \delta\dot{u}_{str} \end{Bmatrix} =
\begin{bmatrix}
\frac{\partial L_1}{\partial\Omega} & 0 & \frac{\partial L_1}{\partial\beta} & 0 & \frac{\partial L_1}{\partial u_{act,0}} & 0 \\
1 & 0 & 0 & 0 & 0 & 0 \\
\frac{\partial L_3}{\partial\Omega} & \frac{\partial L_3}{\partial\Phi} & \frac{\partial L_3}{\partial\beta} & 0 & 0 & 0 \\
0 & 0 & 0 & \frac{\partial\mathcal{F}_1}{\partial U_{\infty ref}} & 0 & 0 \\
\frac{\partial\mathcal{F}_2}{\partial\Omega} & 0 & \frac{\partial\mathcal{F}_2}{\partial\beta} & \frac{\partial\mathcal{F}_2}{\partial U_{\infty ref}} & \frac{\partial\mathcal{F}_2}{\partial u_{act}} & \frac{\partial\mathcal{F}_2}{\partial u_{str}} \\
\frac{\partial\mathcal{F}_3}{\partial\Omega} & 0 & \frac{\partial\mathcal{F}_3}{\partial\beta} & \frac{\partial\mathcal{F}_3}{\partial U_{\infty ref}} & \frac{\partial\mathcal{F}_3}{\partial u_{act}} & \frac{\partial\mathcal{F}_3}{\partial u_{str}}
\end{bmatrix}
\begin{Bmatrix} \delta\Omega \\ \delta\Phi \\ \delta\beta \\ \delta U_{\infty ref} \\ \delta u_{act} \\ \delta u_{str} \end{Bmatrix} +
\begin{bmatrix}
-\frac{\partial L_1}{\partial U_{surge,0}} & 0 \\
0 & 0 \\
0 & -1 \\
\frac{\partial\mathcal{F}_1}{\partial U_{surge}} & 0 \\
\frac{\partial\mathcal{F}_2}{\partial U_{surge}} & 0 \\
0 & 0
\end{bmatrix}
\begin{Bmatrix} \delta U_{surge} \\ K_I N_{gear}\Omega_0 \end{Bmatrix}
$$

(15)

## 3. Results and discussion

### 3.1. PID controller and dynamic inflow verification

This section is to validate the PID controller and the continuous-form state-space dynamic inflow model. Firstly, state-space PID controller(Eq.1,6,and 7) is verified using a time domain test, as shown in Fig.2a, the power keeps stable relying on the controller, which can account for the effectiveness of the PID controller in regulating the power. In addition, fluctuation in Fig.2a is induced by surge motion.

As shown in Eq.11 and 12, two expressions of the dynamic inflow model are given, and if given an excitation, their results of $u_{act}$ are shown in Fig.2b, of which the solid line in blue corresponds to the Eq.11 from Ref. [5], while the dashed line in red represents the response based on Eq.12 proposed in this paper. Results confirm the accuracy of the proposed dynamic inflow model with state-space formula.
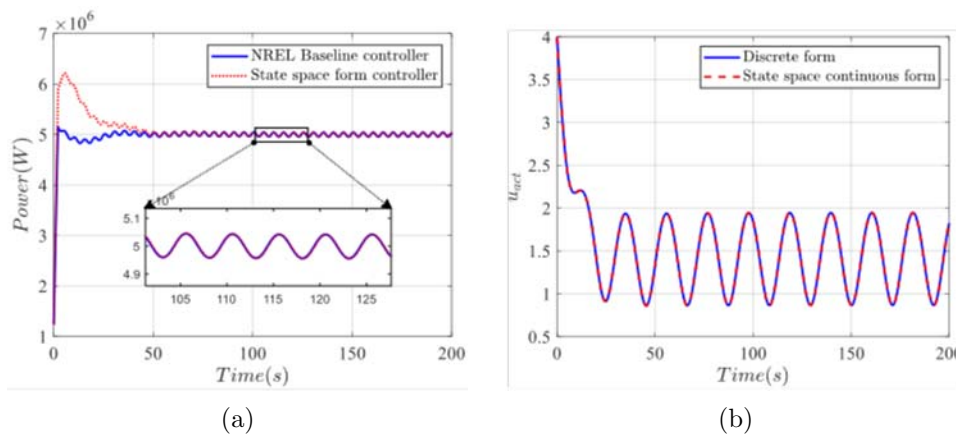


Figure 2: Validations:(a) Validation of PID controller in state space; (b) Validating the continuous state space formulation of dynamic inflow(dashed red line) against Ref. [5] (solid blue line)
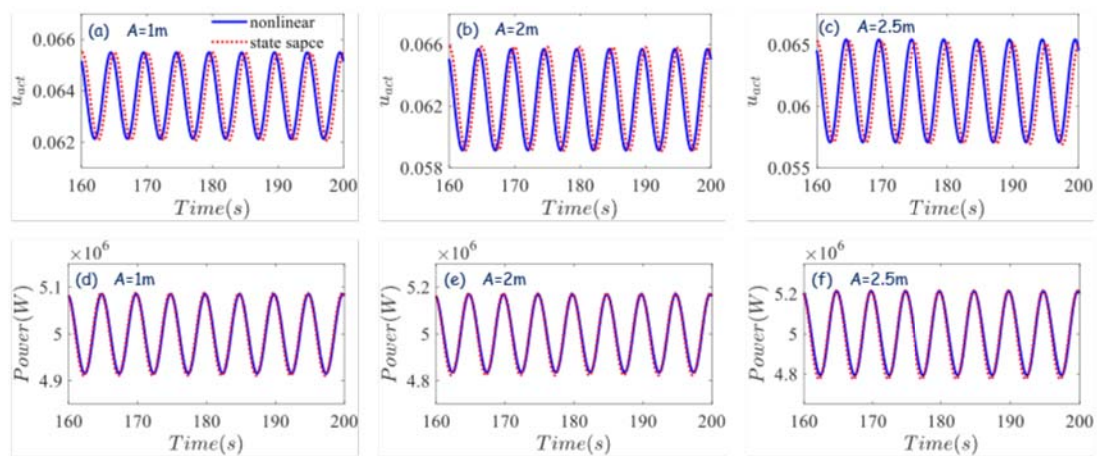
Figure 3: Validation of state space fomulation under various platform surge movements: $T = 5s$, $A = 1, 2,$ and $2.5m$
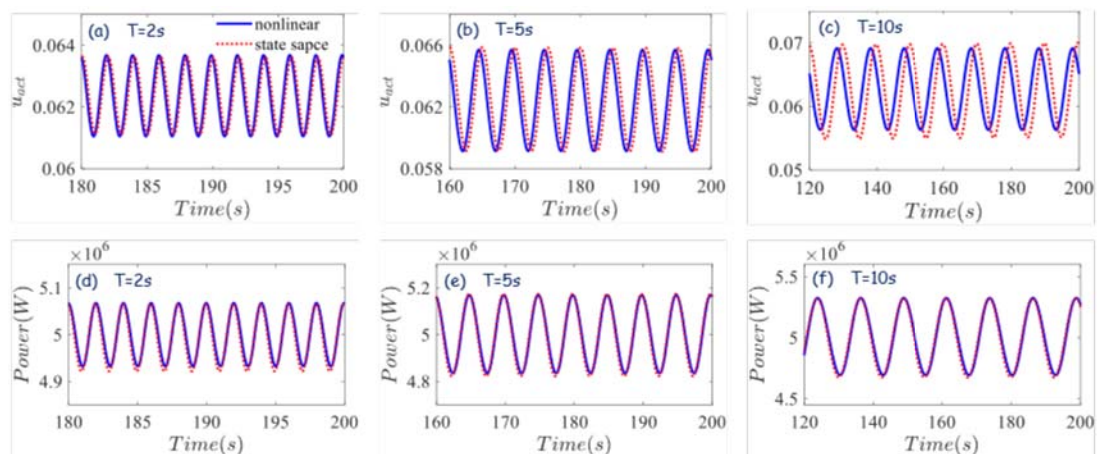


Figure 4: Validation of state space fomulation under various platform surge movements: $A = 2m$, $T = 2, 5,$ and $10s$

*3.2. Model verification on integrated state-space model*

This section presents a bunch of results to validate the proposed overall linear model and methodology provided in Section 2.4. Several cases are designed to observe the accuracy and capability of predicting power outputs. The inflow wind speed is given as 15m/s(Region 3 in Fig.1), and a sinusoidal vibration of platform surge motion is defined as: $A \sin \omega t$, where $A$ is chosen as 0.5, 2, and 2.5m; $\omega = 2\pi/T$, and $T = 5s$. The resulting time series power and induction velocity data are shown in Fig.3. From this, we can observe that a satisfying agreement has been achieved. Identifying the accuracy of the state-space model in predicting the FOWT states under different surge movement amplitudes.

Conversely, to confirm the accuracy of the proposed state-space model under different surge motion frequencies, several tests are conducted, with the amplitude of surge oscillation $A$ as 2m and the oscillation periods $T$ designed as 2, 5, and 10s. Their final simulation data is shown in Fig.4, results confirm the model's ability to predict the power outputs under different surge frequencies, and the higher the frequency, the more accurate the linear model is, especially in the dynamic induction prediction.

In general, with the increase in oscillation amplitude $A$ and period $T$, errors in both amplitudes and phases increase simultaneously.

### 3.3. Prospect

Although the nonlinear wind turbine dynamic model can provide more accurate results and can deal with more complicated circumstances, the linearized one in state space remains irreplaceable. The proposed state-space model is expected to answer some of the scientific questions mentioned in the introduction and is favorable to providing novel insight into PID performance enhancement considering aerodynamic unsteadiness.

## 4. Conclusion

This paper first introduces a widely used nonlinear PID pitch controller model and linearizes this model employing first-order Taylor's expansion. A time-discrete version of the dynamic inflow model accounting for large surge motion-caused aerodynamic unsteadiness is further introduced. Moreover, the introduced dynamic inflow model is transferred into the time-continuous format and is finally linearized step by step using Taylor's expansion. The proposed equations are ultimately assembled in state space, and their capability and accuracy have been validated through time-domain data. The fluctuation of power output and dynamic induction due to platform surge oscillation, specifically both the amplitude and phase can achieve decent agreement with the nonlinear version. However, the discrepancy increases with the increase in surge speed fluctuations.

The newly developed state-space model enables mechanism investigation of the interactions between the pitch controller and the unsteadiness of aerodynamics, which will be further explored. However, the work in this manuscript is still very preliminary and far from any field verification.

### References

[1] Wang, Feng, et al. "GWTSP: A multi-state prediction method for short-term wind turbines based on GAT and GL." Procedia Computer Science 221 (2023): 963-970.
[2] Pustina, L., et al. "Control of power generated by a floating offshore wind turbine perturbed by sea waves." Renewable and Sustainable Energy Reviews 132 (2020): 109984.
[3] Mancini, Simone, et al. "Characterization of the unsteady aerodynamic response of a floating offshore wind turbine." Wind Energy Science Discussions 2020 (2020): 1-26.
[4] Chen, Ziwen, et al. "Numerical analysis of unsteady aerodynamic performance of floating offshore wind turbine under platform surge and pitch motions." Renewable Energy 163 (2021): 1849-1870.
[5] Ferreira, Carlos, et al. "Dynamic inflow model for a floating horizontal axis wind turbine in surge motion." Wind Energy Science 7.2 (2022): 469-485.
[6] Lackner, Matthew A., and Gijs AM van Kuik. "The performance of wind turbine smart rotor control approaches during extreme loads." (2010): 011008.
[7] Hansen, Martin. Aerodynamics of wind turbines. Routledge, 2015.
[8] Jonkman, Jason, et al. Definition of a 5-MW reference wind turbine for offshore system development. No. NREL/TP-500-38060. National Renewable Energy Lab.(NREL), Golden, CO (United States), 2009.
[9] Wright, Allan D., and L. J. Fingersh. Advanced control design for wind turbines; Part I: control design, implementation, and initial tests. No. NREL/TP-500-42437. National Renewable Energy Lab.(NREL), Golden, CO (United States), 2008.

## Appendix A

Derivation of partial derivatives in PID controller:

Firstly write down the d$S$:

$$\mathrm{d}S(\Omega, \beta, u_{act}, U_{surge}) = \frac{1}{2}\rho c \left[ (U_\infty - u_{act} - U_{surge})^2 + (r\Omega)^2 (1 + a')^2 \right] C_t dr \qquad (16)$$

or

$$\mathrm{d}S(\Omega, \beta, u_{act}, U_{surge}) = \frac{1}{2}\rho c \left[ U_\infty^2 (1-a)^2 + U_{surge}^2 - 2U_{surge}U_\infty(1-a) + (r\Omega)^2 (1 + a')^2 \right] C_t dr \qquad (17)$$

in which, $C_t = C_t(\Omega, \beta, u_{act}, U_{surge})$

similarly, d$T$ can be also given as:

$$\mathrm{d}T(\Omega, \beta, u_{act}, U_{surge}) = \frac{1}{2}\rho c \left[ U_\infty^2 (1-a)^2 + U_{surge}^2 - 2U_{surge}U_\infty(1-a) + (r\Omega)^2 (1+a')^2 \right] C_n dr \quad (18)$$

where, $C_n = C_n(\Omega, \beta, u_{act}, U_{surge})$

besides, induction factors are provided as:

$$a = \frac{1}{\frac{4\sin^2\phi}{\sigma C_n} + 1}, \quad a' = \frac{1}{\frac{4\sin\phi\cos\phi}{\sigma C_t} - 1} \quad (19)$$

and force coefficients in two orthogonal directions can be projected as:

$$C_t = C_l \sin\phi - C_d \cos\phi, \quad C_n = C_l \cos\phi + C_d \sin\phi \quad (20)$$

where $C_l$ and $C_d$ is the lift and drag coefficients respectively, and considering the FOWT platform velocity:

$$\tan\phi = \frac{U_\infty(1-a) - U_{surge}}{r\Omega(1+a')} = \frac{U_\infty - u_{act} - U_{surge}}{r\Omega(1+a')} \quad (21)$$

Firstly, $\frac{\partial(\mathrm{d}S)}{\partial U_{surge}}$ can be written as

$$\frac{\partial(\mathrm{d}S)}{\partial U_{surge}} = \frac{1}{2}\rho c \cdot dr \cdot \left[ \frac{\partial\left(V_{Rel}^2\right)}{\partial U_{surge}} C_t + V_{Rel}^2 \frac{\partial C_t}{\partial U_{surge}} \right] \quad (22)$$

Similarly,

$$\frac{\partial(\mathrm{d}S)}{\partial u_{act}} = \frac{1}{2}\rho c \cdot dr \cdot \left[ \frac{\partial\left(V_{Rel}^2\right)}{\partial u_{act}} C_t + V_{Rel}^2 \frac{\partial C_t}{\partial u_{act}} \right], \quad \frac{\partial(dS)}{\partial \Omega} = \frac{1}{2}\rho c \cdot dr \cdot \left[ \frac{\partial\left(V_{Rel}^2\right)}{\partial \Omega} C_t + V_{Rel}^2 \frac{\partial C_t}{\partial \Omega} \right]$$
$$\frac{\partial(dS)}{\partial \beta} = \frac{1}{2}\rho c \cdot dr \cdot \left[ \frac{\partial\left(V_{Rel}^2\right)}{\partial \beta} C_t + V_{Rel}^2 \frac{\partial C_t}{\partial \beta} \right] \quad (23)$$

besides,

$$\frac{\partial(dT)}{\partial \Omega} = \frac{1}{2}\rho c \cdot dr \cdot \left[ \frac{\partial\left(V_{Rel}^2\right)}{\partial \Omega} C_n + V_{Rel}^2 \frac{\partial C_n}{\partial \Omega} \right], \quad \frac{\partial(dT)}{\partial \beta} = \frac{1}{2}\rho c \cdot dr \cdot \left[ \frac{\partial\left(V_{Rel}^2\right)}{\partial \beta} C_n + V_{Rel}^2 \frac{\partial C_n}{\partial \beta} \right] \quad (24)$$

Thus, items to be derived can be listed as: $\frac{\partial\left(V_{Rel}^2\right)}{\partial U_{surge}}, \frac{\partial\left(V_{Rel}^2\right)}{\partial u_{act}}, \frac{\partial\left(V_{Rel}^2\right)}{\partial \Omega}, \frac{\partial\left(V_{Rel}^2\right)}{\partial \beta}, \frac{\partial C_t}{\partial U_{surge}}, \frac{\partial C_t}{\partial u_{act}}, \frac{\partial C_t}{\partial \Omega}$, $\frac{\partial C_t}{\partial \beta}, \frac{\partial C_n}{\partial \Omega}, \frac{\partial C_n}{\partial \beta}$

Relative wind speed is expressed:

$$V_{Rel}^2 = U_\infty^2 (1-a)^2 + U_{surge}^2 - 2U_{surge}U_\infty(1-a) + (r\Omega)^2 (1+a')^2$$
$$= (U_\infty - u_{act} - U_{surge})^2 + (r\Omega)^2 (1+a')^2 \quad (25)$$

The expression for above-mentioned terms can be expressed as follows:

$$\frac{\partial\left(V_{Rel}^2\right)}{\partial U_{surge}} = 2U_{surge} - 2U_\infty(1-a) + 2\left[U_{surge}U_\infty - U_\infty^2(1-a)\right]\frac{\partial a}{\partial U_{surge}} + 2r^2\Omega^2(1+a')\frac{\partial a'}{\partial U_{surge}}$$

$$\frac{\partial\left(V_{Rel}^2\right)}{\partial u_{act}} = -2(U_\infty - u_{act} - U_{surge})$$

$$\frac{\partial\left(V_{Rel}^2\right)}{\partial \Omega} = -2U_\infty^2(1-a)\frac{\partial a}{\partial \Omega} + 2U_{surge}U_\infty\frac{\partial a}{\partial \Omega} + 2r^2\Omega(1+a')^2 + 2r^2\Omega^2(1+a')\frac{\partial a'}{\partial \Omega} \quad (26)$$

$$\frac{\partial\left(V_{Rel}^2\right)}{\partial \beta} = -2U_\infty^2(1-a)\frac{\partial a}{\partial \beta} + 2U_{surge}U_\infty\frac{\partial a}{\partial \beta} + 2r^2\Omega^2(1+a')\frac{\partial a'}{\partial \beta}$$

in which,

$$
\frac{\partial a}{\partial U_{surge}} = \frac{da}{d\phi} \cdot \frac{\partial \phi}{\partial U_{surge}}, \quad \frac{\partial a'}{\partial U_{surge}} = \frac{da'}{d\phi} \cdot \frac{\partial \phi}{\partial U_{surge}}, \quad \frac{\partial a}{\partial \Omega} = \frac{da}{d\phi} \cdot \frac{\partial \phi}{\partial \Omega}, \quad \frac{\partial a'}{\partial \Omega} = \frac{da'}{d\phi} \cdot \frac{\partial \phi}{\partial \Omega},
$$
$$
\frac{\partial a}{\partial \beta} = \frac{\partial a}{\partial C_n} \frac{\partial C_n}{\partial \alpha} \frac{\partial \alpha}{\partial \beta} = -\frac{\partial a}{\partial C_n} \left( \frac{\partial C_l}{\partial \alpha} \cos \phi + \frac{\partial C_d}{\partial \alpha} \sin \phi \right) \tag{27}
$$
$$
\frac{\partial a'}{\partial \beta} = \frac{\partial a'}{\partial C_t} \frac{\partial C_t}{\partial \alpha} \frac{\partial \alpha}{\partial \beta} = -\frac{\partial a'}{\partial C_t} \left( \frac{\partial C_l}{\partial \alpha} \sin \phi - \frac{\partial C_d}{\partial \alpha} \cos \phi \right)
$$

where $\frac{da}{d\phi}$ and $\frac{da'}{d\phi}$ can be determined from as:

$$
\frac{da}{d\phi} = \frac{-4 \left( \sin 2\phi C_n - \frac{dC_n}{d\phi} \sin^2 \phi \right)}{\sigma C_n^2 \left( \frac{4\sin^2 \phi}{\sigma C_n} + 1 \right)^2}, \quad \frac{da'}{d\phi} = \frac{-4 \left( \cos 2\phi C_t - \frac{dC_t}{d\phi} \sin \phi \cos \phi \right)}{\sigma C_t^2 \left( \frac{4\sin \phi \cos \phi}{\sigma C_t} - 1 \right)^2} \tag{28}
$$

The expressions for $\frac{\partial \phi}{\partial U_{surge}}$ and $\frac{\partial \phi}{\partial \Omega}$ can be found from above equations using:

$$
\frac{\partial \left( \tan \phi \cdot r\Omega \left( 1 + a' \right) \right)}{\partial \phi} \frac{\partial \phi}{\partial U_{surge}} = \frac{\partial \left( U_\infty (1 - a) \right)}{\partial \phi} \frac{\partial \phi}{\partial U_{surge}} - 1 \tag{29}
$$

expand the equation above,

$$
\frac{\partial \phi}{\partial U_{surge}} \left( \sec^2 \phi \cdot r\Omega \left( 1 + a' \right) + \tan \phi \cdot r\Omega \frac{\partial a'}{\partial \phi} + U_\infty \frac{\partial a}{\partial \phi} \right) = -1 \tag{30}
$$

and,

$$
\frac{\partial \phi}{\partial \Omega} \left[ \frac{d \left( \frac{1-a}{1+a'} \right)}{d\phi} \cot \phi - \frac{1}{\sin^2 \phi} \cdot \frac{1-a}{1+a'} \right] = \frac{r}{U_\infty} \tag{31}
$$

where $\frac{d \left( \frac{1+a'}{1-a} \right)}{d\phi} = \frac{\frac{da'}{d\phi}(1-a) + \frac{da}{d\phi}(1+a')}{(1-a)^2}$.

Additionally,

$$
\frac{\partial a}{\partial C_n} = \left( \frac{4\sin^2 \phi}{\sigma C_n} + 1 \right)^{-2} \frac{4\sin^2 \phi}{\sigma} \frac{1}{C_n^2}, \quad \frac{\partial a'}{\partial C_t} = \left( \frac{4\sin \phi \cos \phi}{\sigma C_t} - 1 \right)^{-2} \frac{4\sin \phi \cos \phi}{\sigma} \frac{1}{C_t^2} \tag{32}
$$

A second set of derivatives are:

$$
\frac{\partial C_t}{\partial U_{surge}} = \frac{\partial C_t}{\partial \phi} \frac{\partial \phi}{\partial U_{surge}}, \quad \frac{\partial C_t}{\partial u_{act}} = \frac{\partial C_t}{\partial \phi} \frac{\partial \phi}{\partial u_{act}}, \quad \frac{\partial C_t}{\partial \Omega} = \frac{\partial C_t}{\partial \phi} \frac{\partial \phi}{\partial \Omega}
$$
$$
\frac{\partial C_t}{\partial \beta} = \frac{\partial C_t}{\partial \alpha} \frac{\partial \alpha}{\partial \beta}, \quad \frac{\partial C_n}{\partial \Omega} = \frac{\partial C_n}{\partial \phi} \frac{\partial \phi}{\partial \Omega}, \quad \frac{\partial C_n}{\partial \beta} = \frac{\partial C_n}{\partial \alpha} \frac{\partial \alpha}{\partial \beta} \tag{33}
$$

in which,

$$
\frac{dC_t}{d\phi} = \frac{\partial C_l}{\partial \phi} \sin \phi - \frac{\partial C_d}{\partial \phi} \cos \phi + C_l \cos \phi + C_d \sin \phi
$$
$$
\frac{dC_n}{d\phi} = \frac{\partial C_l}{\partial \phi} \cos \phi + \frac{\partial C_d}{\partial \phi} \sin \phi - C_l \sin \phi + C_d \cos \phi \tag{34}
$$

and,

$$
\frac{\partial \left( \tan \phi \cdot r\Omega \left( 1 + a' \right) \right)}{\partial \phi} \frac{\partial \phi}{\partial u_{act}} = -1 \tag{35}
$$

expand,

$$
\frac{\partial \phi}{\partial u_{act}} \left( \sec^2 \phi \cdot r\Omega \left( 1 + a' \right) + \tan \phi \cdot r\Omega \frac{\partial a'}{\partial \phi} \right) = -1 \tag{36}
$$

## Appendix B

Partial derivatives in dynamic inflow model:

$$\frac{\partial \mathcal{F}_1}{\partial U_{\infty ref}} = (U_\infty - U_{surge0} - U_{\infty ref0}) e^{-f_0} L_{str}^{-1} + \frac{1}{\Delta t}\left(1 - e^{-f^0}\right) \tag{37}$$

$$\frac{\partial \mathcal{F}_1}{\partial U_{surge}} = -\frac{1}{\Delta t}\left(e^{-f^0} - 1\right) \tag{38}$$

$$\frac{\partial \mathcal{F}_2}{\partial U_{\infty ref}} = -\frac{1}{\Delta t}e^{\frac{\Delta t}{\tau_{act10}}}\left(1 - e^{-\frac{\Delta t}{\tau_{act20}}}\right)\frac{C_{T0}U_\infty^2}{4}U_{str0}^{-2} + e^{\frac{\Delta t}{\tau_{act10}}}u_{qs0}e^{-\frac{\Delta t}{\tau_{act20}}}\frac{1}{L_{act}} \tag{39}$$

$$\begin{aligned}\frac{\partial \mathcal{F}_2}{\partial u_{act}} = &\frac{1}{\Delta t}\left(1 - e^{\frac{\Delta t}{\tau_{act10}}}\right) - \frac{1}{2}\left(\left(1 - e^{-\frac{\Delta t}{\tau_{act20}}}\right)u_{qs0} - u_{act0}(t)\right)e^{\frac{\Delta t}{\tau_{act10}}}\frac{1}{L_{act}}\\ &- \frac{1}{2}e^{\frac{\Delta t}{\tau_{act10}}}u_{qs0}e^{-\frac{\Delta t}{\tau_{act20}}}\frac{1}{L_{act}} + \frac{1}{2\Delta t}e^{\frac{\Delta t}{\tau_{act10}}}\left(1 - e^{-\frac{\Delta t}{\tau_{act20}}}\right)\frac{C_{T0}U_\infty^2}{4}U_{str0}^{-2}\end{aligned} \tag{40}$$

$$\frac{\partial \mathcal{F}_2}{\partial u_{str}} = \frac{1}{2\Delta t}e^{\frac{\Delta t}{\tau_{act10}}}\left(1 - e^{-\frac{\Delta t}{\tau_{act20}}}\right)\frac{C_{T0}U_\infty^2}{4}U_{str0}^{-2} \tag{41}$$

$$\frac{\partial \mathcal{F}_2}{\partial U_{surge}} = -\left(\left(1 - e^{-\frac{\Delta t}{\tau_{act20}}}\right)u_{qs0} - u_{act0}(t)\right)e^{\frac{\Delta t}{\tau_{act10}}}\frac{1}{L_{act}} \tag{42}$$

$$\begin{aligned}\frac{\partial \mathcal{F}_2}{\partial \Omega} = &\{A + B + C\}\int_0^R \frac{\partial a}{\partial \Omega} + \frac{1}{\Delta t}e^{\frac{\Delta t}{\tau_{act10}}}\left(1 - e^{-\frac{\Delta t}{\tau_{act20}}}\right)\frac{U_\infty^2}{4}\frac{1}{U_{str0}}\frac{2}{\rho U_{\infty ref0}^2 \pi R^2}\int_0^R \frac{\partial \mathrm{d}T}{\partial \Omega}\\ A = &-\frac{U_\infty}{2L_{act}}\left(\left(1 - e^{-\frac{\Delta t}{\tau_{act20}}}\right)u_{qs0} - u_{act0}(t)\right)e^{\frac{\Delta t}{\tau_{act10}}},\ B = \frac{U_\infty}{\Delta t}\left(1 - e^{\frac{\Delta t}{\tau_{act10}}}\right) - \frac{U_\infty}{2L_{act}}e^{\frac{\Delta t}{\tau_{act10}} - \frac{\Delta t}{\tau_{act20}}}u_{qs0}\\ C = &\frac{1}{\Delta t}e^{\frac{\Delta t}{\tau_{act10}}}\left(1 - e^{-\frac{\Delta t}{\tau_{act20}}}\right)\frac{C_{T0}U_\infty^2}{4}U_{str0}^{-2}\frac{U_\infty}{2}\end{aligned} \tag{43}$$

$$\frac{\partial \mathcal{F}_2}{\partial \beta} = \{A + B + C\}\int_0^R \frac{\partial a}{\partial \beta} + \frac{1}{\Delta t}e^{\frac{\Delta t}{\tau_{act10}}}\left(1 - e^{-\frac{\Delta t}{\tau_{act20}}}\right)\frac{U_\infty^2}{4}\frac{1}{U_{str0}}\frac{2}{\rho U_{\infty ref0}^2 \pi R^2}\int_0^R \frac{\partial \mathrm{d}T}{\partial \beta} \tag{44}$$

$$\frac{\partial \mathcal{F}_3}{\partial U_{\infty ref}} = (u_{qs0} - u_{str0}(t))e^{\frac{\Delta t}{\tau_{str0}}}\frac{1}{L_{str}} - \frac{1}{\Delta t}\left(e^{\frac{\Delta t}{\tau_{str0}}} - 1\right)\frac{C_{T0}U_\infty^2}{4}U_{str0}^{-2} \tag{45}$$

$$\frac{\partial \mathcal{F}_3}{\partial u_{act}} = -(u_{qs0} - u_{str0}(t))e^{\frac{\Delta t}{\tau_{str0}}}\frac{1}{2L_{str}} + \frac{1}{2\Delta t}\left(e^{\frac{\Delta t}{\tau_{str0}}} - 1\right)\frac{C_{T0}U_\infty^2}{4}U_{str0}^{-2} \tag{46}$$

$$\frac{\partial \mathcal{F}_3}{\partial u_{str}} = \frac{1}{\Delta t}\left(1 - e^{\frac{\Delta t}{\tau_{str0}}}\right) + \frac{1}{2\Delta t}\left(e^{\frac{\Delta t}{\tau_{str0}}} - 1\right)\frac{C_{T0}U_\infty^2}{4}U_{str0}^{-2} \tag{47}$$

$$\begin{aligned}\frac{\partial \mathcal{F}_3}{\partial \Omega} = &-(u_{qs0} - u_{str0}(t))e^{\frac{\Delta t}{\tau_{str0}}}\frac{U_\infty}{2L_{str}}\int_0^R \frac{\partial a}{\partial \Omega}\\ &+ \frac{1}{\Delta t}\left(e^{\frac{\Delta t}{\tau_{str0}}} - 1\right)\left(\frac{U_\infty^2}{4}\frac{1}{U_{str0}}\frac{2}{\rho U_{\infty ref0}^2 \pi R^2}\int_0^R \frac{\partial \mathrm{d}T}{\partial \Omega} + \frac{C_{T0}U_\infty^3}{8}U_{str0}^{-2}\int_0^R \frac{\partial a}{\partial \Omega}\right)\end{aligned} \tag{48}$$

$$\begin{aligned}\frac{\partial \mathcal{F}_3}{\partial \beta} = &-(u_{qs0} - u_{str0}(t))e^{\frac{\Delta t}{\tau_{str0}}}\frac{U_\infty}{2L_{str}}\int_0^R \frac{\partial a}{\partial \beta}\\ &+ \frac{1}{\Delta t}\left(e^{\frac{\Delta t}{\tau_{str0}}} - 1\right)\left(\frac{U_\infty^2}{4}\frac{1}{U_{str0}}\frac{2}{\rho U_{\infty ref0}^2 \pi R^2}\int_0^R \frac{\partial \mathrm{d}T}{\partial \beta} + \frac{C_{T0}U_\infty^3}{8}U_{str0}^{-2}\int_0^R \frac{\partial a}{\partial \beta}\right)\end{aligned} \tag{49}$$

The '0' in the subscript of the above formulas represents the variable value of the previous iteration.